Available online at www.sciencedirect.com
ScienceDirect
Journal of Bionic Engineering 14 (2017) 506–519

# Application of Bioinspired Superhydrophobic Surfaces in Two-phase Heat Transfer Experiments

**Emanuele Teodori[1], Ana Sofia Moita[1], Miguel Moura[1], Pedro Pontes[1], António Moreira[1], Yuan Bai[2], Xinlin Li[2], Yan Liu[2]**

1. *IN+– Center for Innovation, Technology and Policy Research, Instituto Superior Técnico, Universidade de Lisboa, Av. Rovisco Pais*, 1049-001 *Lisboa*, *Portuga*
2. *Key Laboratory of Bionic Engineering* (*Ministry of Education*), *Jilin University*, *Changchun* 130022, *China*

**Abstract**

This paper addresses the potential to use Lotus leaf bioinspired surfaces in applications involving heat transfer with phase change, namely pool boiling and spray impingement. Besides describing the role of bioinspired topographical features, using an innovative technique combining high-speed visualization and time-resolved infrared thermography, surface durability is also addressed. Water is used for pool boiling and for spray impingement systems (simplified as single droplet impact), while HFE7000 is used in a pool boiling cooler for electronic components. Results show that surface durability is quickly compromised for water pool boiling applications, as the chemical treatment does not withstand high temperatures ($T > 100$ ˚C) during long time intervals (3 h – 4 h). For HFE7000 pool boiling (depicting lower saturation temperature − 34 ˚C), heat transfer enhancement is governed by the topography. The regular hierarchical pattern of the bioinspired surfaces promotes the heat transfer coefficient to increase up to 22.2%, when compared to smooth surfaces, while allowing good control of the interaction mechanisms until a distance between micro-structures of 300 μm – 400 μm. Droplet impingement was studied for surface temperatures ranging between 60 ˚C – 100 ˚C. The results do not support the use of superhydrophobic surfaces for cooling applications, but reveal great potential for other applications involving droplet impact on heated surfaces (*e.g.* metallurgy industry).

**Keywords:** bioinspired surfaces, surface micro-patterning, two-phase heat transfer, time resolved infrared thermography


doi: 10.1016/S1672-6529(16)60417-1

## 1 Introduction

The categorization of the wetting regimes is still debated, but it is usually accepted that superhydrophobic surfaces have equilibrium contact angles larger than 150˚ and a hysteresis (*i.e.* the difference between the quasi-static advancing and receding angle) lower than 10˚. Conversely, hydrophilic surfaces (*i.e.* attracting water) have contact angles lower than 90˚. Superhydrophilicity is often considered for contact angles lower than 10˚[1]. Superhydrophobic surfaces are important in many industrial applications, *e.g.* Refs. [2] and [3]. Despite the variety of surfaces available, they are not always designed to cope with the actual needs. Biological surfaces, in contrast, depict high functionality, as they are optimized to perfectly fit to the desired functions. For instance, the Lotus leaf is still an impressive example of a superhydrophobic surface with high self-cleaning ability, which is strongly related to its micro- and nano- roughness[4]. Interesting superhydrophobic properties have also been identified for instance in rose petals[5] and more recently in English weed leaves[6]. Effective identification and transfer of the properties related to these features is not easy and additional complexity arrives when the surfaces are subjected to demanding conditions, which may compromise their durability. For instance, surface wettability is known to play a vital role in cooling applications with liquid phase change, but the durability of the chemical treatment is often a problem[7]. Microprocessors thermal management is argued to be the largest limitation to the development of new processors in the near future, which

**Corresponding author:** Ana Sofia Moita
**E-mail:** anamoita@tecnico.ulisboa.pt

demands for innovative cooling strategies. Two of the most popular cooling strategies which are currently being explored involve liquid phase change and are based on pool boiling (*e.g.* Refs. [8] and [9]) or on spray impingement (*e.g.* Refs. [10] and [11]). For safety reasons, these systems usually work with dielectric fluids, which have lower thermophysical properties than more common and inexpensive fluids, such as water. To cope with this limitation, the use of structured surfaces and/or surfaces with custom made wettability in this kind of systems was investigated by *e.g.* Ref. [9] who confirmed the benefits achievable by using structured surfaces in enhancing the pool boiling heat transfer. However no direct link was proposed between the fundamental studies of the effect of the surface structure and the application of interest. In this context, difficulties are related to the fact that most hydrophobic surfaces cannot hold very high temperatures, such as those achieved in many pool boiling systems for cooling purposes. Hence, the present study addresses droplet impact and pool boiling as two relevant case studies of cooling applications which may take advantage of the bioinspired surfaces devised here to improve the heat transfer. Droplet impact is taken as a simplified approach to spray cooling. This is actually not so far from the real systems for microelectronics cooling, which actually deal with single droplets or with very sparse sprays[12], for which interaction mechanisms (*e.g.* droplet-droplet interactions) are less prominent.

Concerning pool boiling heat transfer, previous studies reported in the literature[13,14] are consistent in the description of the effect of wettability: for superhydrophobic surfaces, bubble nucleation starts at low superheat values (1 K – 3 K), given that the energy barrier necessary for nucleus generation is smaller. However, despite nucleation is favoured, the generated bubbles tend to stay attached on the surface, growing and promoting coalescence, leading to the formation of large vapour films that insulate the surface. This boiling behaviour leads to low heat fluxes removable by this kind of surfaces when compared to hydrophilic ones. On the other hand, hydrophilic or superhydrophilic surfaces require larger superheat to start bubble nucleation, but facilitate bubbles release. Following these observations, few authors[15] suggest the development of the so-called biphilic surfaces, *i.e.* superhydrophilic surfaces with superhydrophobic regions and report a significant enhancement of the heat flux that can be removed from these surfaces[16]. However, the design of an optimum pattern is still far to be achieved and requires a deeper study on the fluid dynamics and heat transfer processes that govern the observed phenomena[17]. Also, despite these encouraging results, there is still a strong concern related to the most adequate process to produce the surfaces, which must be assessed according to the particular case of interest, as it may strongly affect the application for which the surface is devised in many unexpected ways. In fact, modification of surface wettability, namely to create superhydrophobic characteristics requires combining techniques to alter the surface topography (*e.g.* chemical etching[18], plasma enhanced chemical vapour deposition[19], anodic oxidization[20] and sol−gel[21]) with chemical modification using low-surface energy materials. However, when dealing with pool boiling heat transfer, these procedures affect the boiling dynamics and consequently the heat transfer in a different way. Hence, while modifying the wettability at the expense of changing the surface chemistry, mainly acts on the onset of boiling and on the bubble release mechanisms, surface topography can simultaneously alter the wettability and the nucleation sites density, as well as strongly affect the interaction mechanisms[22]. It is known that micro-patterning the surface can improve the cooling performance of a system based on pool boiling *e.g.* Ref. [23]. Despite complex geometries were proposed in the literature, several authors *e.g.* Refs. [24–26] confirmed that arrays of etched cavities on the surface were an effective simple geometry capable of increasing the heat transfer coefficient up to 150%. Such enhancement results from the combined effect of the surface augmentation (increase of the contact area) and the promotion of the heterogeneous nucleation process by means of the etched cavities. However, these two parameters do not affect linearly the heat transfer coefficient. In fact, interaction mechanisms can be promoted decreasing the spacing between cavities and this can affect the boiling process. In particular, when horizontal coalescence occurs intensively, a corresponding degradation of the heat transfer coefficient was noticed.

Wettability also plays a vital role in droplet impact for cooling applications. For instance, Refs. [27] and [28] report that surface topography, wettability and liquid properties interact in a complex way to alter the wetting

behaviour of droplets impacting at different surface temperatures. After impact, the droplet spreads radially over the surface in a process dominated by inertial forces until it reaches a maximum diameter in which these forces are balanced by surface tension and viscosity. To minimize its surface energy, the droplet recedes, being this motion repeated until equilibrium is reached. If the inertial forces immediately overcome the cohesive action of the surface tension, disintegration occurs, by a variety of mechanisms, which also depend on liquid and surface properties, on wettability and on topography[28]. For impacts on superhydrophobic surfaces, air is often entrapped between the surface and the droplets and between the rough groves of the surfaces[12], thus favouring the spreading and reducing the action of viscous forces near the surface. The so-called pinning of the contact line is also often reduced, thus further limiting the energy dissipation at the contact line. Consequently, the surface energy of the droplet at its maximum extent is high enough to favour the fast droplet recoil followed by a partial or complete rebound[29]. The actual governing mechanisms are however still not well described and despite the large number of studies focusing on droplet impact on surfaces, still rudimentary understanding is achieved when complex surfaces with modified topography and/or chemistry are used[30]. This knowledge is even sparser when the complexity of the surfaces includes hierarchical structures, such as those present in biomimetic surfaces, which requires demanding static and dynamic wetting characterization methodologies, as recently reported by Ref. [6]. On the other hand, the intricate fluid dynamic and heat transfer processes are very difficult to model and even experimental studies providing quantitative analysis of the heat transfer are scarce, given the particularly demanding experimental conditions and the limitations in the current diagnostic techniques. Few interesting papers provide this kind of quantitative information[31–34] and in most of these studies, the heat transferred during the impact of a droplet onto a heating surface is usually evaluated based on measurements performed with thermocouples placed beneath the heating surface. Improved spatial resolution is achieved using IR (infrared) thermography to obtain the temperature distribution on the heated surface during droplet impact[35] and/or on the droplet itself[36,37] although the later mainly focus on sessile droplets, so the technique still needs further development and validation for more complex dynamic conditions. Particular issues are related to an accurate calibration and to the low temporal resolution provided by many of these IR studies[38].

From the introduction reported here one can identify several topics to solve in the efficient implementation of a complex surface to enhance heat transfer in cooling systems based on liquid phase change. On one hand, the processes studied here (pool boiling and droplet/wall interactions) are still not entirely described and the role of complex surfaces, particularly when dealing with bioinspired structures is still far to be understood. In this context, the fabrication methods must be studied to vary the surface properties in a controlled and systematic way. Durability of the surfaces is also an issue considering the very harsh environment they are subjected to. For cooling systems based on spray/droplet impingement, studies addressing heat transfer are scarce and are limited to the existing diagnostic techniques. In line with this, the present work addresses a systematic study to devise the appropriate surfaces to enhance heat transfer processes with liquid phase change, in the context of an application to electronics cooling. Two cooling strategies are considered, namely pool boiling and spray/droplet impingement. In pool boiling experiments, surface chemistry and topography are addressed in different working conditions and several techniques are tested to prepare the test surfaces. The various surface parameters which are systematically studied are related to the physical processes that govern the observed phenomena. Different fluids are considered, namely water and a dielectric fluid (HFE7000 from 3M) to allow exploring a wider range of wetting properties and evaluate the effect of surface topography in extreme wetting scenarios. Assessment of the durability of the surface treatment, which is often omitted in the literature, plays a vital role in a real application, so it will be addressed here. Similar methodology is then implemented to devise the surfaces used in spray/droplet impingement applications. For this case study, an innovative diagnostic technique is proposed, the time resolved IR thermography, which is combined with high-speed visualization and image post-processing to provide additional information on the actual heat transfer processes occurring at the interface between the droplet and the complex surfaces tested here.

## 2 Materials and methods

### 2.1 Preparation and characterization of the test surfaces

Square surfaces ((60 × 60) $mm^2$) made from an aluminium alloy were used. The composition of this 2024 Al alloy is 4.2 wt.% Cu, 1.5 wt.% Mg, 0.7 wt.% Mn, 0.2 wt.% Fe, and Al. The surfaces bioinspired in the Lotus leaf were prepared following a fabrication method composed by two steps: construction of rough structures followed by chemical modification with low-surface-energy materials. The fabrication of the rough structures was made as follows: first, the samples were abraded using SiC papers (from 800 to 2000 grades), polished to mirror, ultrasonically cleaned for 10 min in absolute ethanol (A.R. Beijing Chemical Works) and then dried under room conditions. Afterwards, the microarray structures were produced by laser etching (FB20-1, New Industries, China). The laser system parameters assessed were the depth and diameter of laser-ablated micro-cavities, the laser beam power and the number of marks of the beam in the same micro-cavity. Chemical treatment involves a solution of toluene (99.5%), DTS ($CH_3(CH_2)_{11}Si(OCH_3)_3$) and absolute ethanol. Keeping the bioinspired micro-pattern, an additional set of sample surfaces was prepared only by laser etching, to focus on the sole effect of the bioinspired pattern. The micro-patterns consist in arrays of circular cavities with 100 μm in diameter and 15 μm in depth. The distance between cavities, $S$ is subjected to a parametric study being varied between 800 μm, 600 μm, 400 μm and 300 μm. A smooth surface is taken as reference. The obtained samples were characterized by Scanning Electron Microscopy (SEM) (JBM-7500F, Japan Electronic). The surface chemical composition was examined by X-ray Photoelectron Spectroscopy (XPS, SPECS XR50). The static water contact angles of the sample surfaces were evaluated using a contact angle meter (JC2000A Powereach, China) based on a sessile drop measuring method using distilled water droplets with a volume of 5 μL. The final values are taken from an average measured at five different points. The surfaces chemically coated have contact angles of 151˚ ± 3˚, with a hysteresis lower than 4˚, so they can be considered superhydrophobic, following the criteria of Ref. [1]. This angle is very similar in all the micro-structured surfaces. For smooth coated aluminium surfaces, the angle obtained here is only slightly lower, 146˚ ± 3˚. The uncoated hydrophilic aluminium smooth surfaces, used here as a reference, depict typical contact angles of 35˚ ± 5˚. The contact angles measured at the micro-structured uncoated region of the surfaces can vary from 45˚ ± 10˚ for the surfaces with the sparser cavities to 100˚ ± 5˚ for the surfaces with smaller distances between cavities, $S$ = 100 μm. The surface roughness indeed alters the wettability but, contrarily to what is stated by the classical theories of Wenzel and of Cassie and Baxter, there is no straightforward relation between the contact angle and the surface topography. These observations are confirmed for instance by Ref. [39]. So, at the scale considered here, the effect of the surface topography in changing the wettability is not negligible but the chemical coating is the responsible for the superhydrophobic behaviour.

### 2.2 Application of the surfaces to the cooling systems

Distilled water and HFE 7000 were the chosen working fluids. Water was used to infer on the superhydrophobicity of the used surfaces and HFE 7000 was chosen due to its dielectric properties and low saturation temperature ($T_{sat}$ = 34 ˚C at 1.01325 bar, Table 1), which are particularly adequate for direct immersion cooling of electronic components. The main thermophysical properties of the fluids are reported in Table 1. In addition, the large difference between the surface tension values of this liquid and of water allows exploring a wider range of wetting properties and evaluating the effect of surface topography in extreme wetting scenarios.

The experimental arrangement used to test the complex surfaces under pool boiling experiments using water is mainly composed by a boiling chamber, a degassing station and a waste tank. The detailed description of this set-up can be found in Ref. [26]. The pool boiling experiments using the dielectric fluid HFE 7000 were performed in a modular two phase close loop thermosiphon, which is being devised to work as a cooling system for microprocessors. Within this scope, a custom made heating system was devised to simulate the thermal behaviour of a real CPU. The detailed description of this heating system and of the experimental procedures to devise it is given in Ref. [9]. Ref. [9] also displays a detailed description of this cooling system, together with a schematic of the full set-up, which is not presented here due to paper length constraints. This

**Table 1** Thermophysical properties of the working fluids at 1.01325 bar

| Property | HFE 7000 | Distilled water |
|---|---|---|
| Saturation Temperature, $T_{sat}$ (˚C) | 34 | 100 |
| Liquid density, $\rho_l$ (kg·m$^{-3}$) | 1374.7 | 957.8 |
| Vapour density, $\rho_v$ (kg·m$^{-3}$) | 4.01 | 0.5956 |
| Liquid dynamic viscosity, $\mu_l$ (mNs·m$^{-1}$) | 0.3437 | 0.279 |
| Specific heat, $Cp_l$ (J·(kg·˚C)$^{-1}$) | 1352.5 | 4217 |
| Thermal conductivity of the fluid, $k_l$ (W·(m·K)$^{-1}$) | 0.07 | 0.68 |
| Latent heat of vaporization, $H_{fg}$ (kJ·kg$^{-1}$) | 142 | 2257 |
| Liquid surface tension, $\sigma_{lv}$ (N·m$^{-1}$)×10$^{-3}$ | 12.4 | 58 |

cooling system is composed by an evaporator and a condenser connected by PVC tubes. The evaporator consists on an Acrylic cylindrical reservoir of 42 mm inner diameter and 40 mm height. The bioinspired surfaces act as interface between the liquid and the CPU heat spreader. Given that the applied chemical treatment does not repel the HFE7000, this set-up was mainly used to study the sole effect of surface micro-patterning, in the absence of extreme wetting scenarios. The vapour mass coming from the evaporator rises and enters into one of the PVC tubes, being transported to the condenser. Then, the condensed liquid is returned from the condenser to the bottom of the evaporator by another PVC tube. The tubes are transparent to allow flow visualization. The PVC tubes are just used to transport the fluid mass between the evaporator and the condenser and do not alter the flow inside the evaporator, so they do not play any role or interference in the experiments presented here. The condenser consists on a flat tube and plain serpentine fins configuration with a frontal area of (120 × 120) mm$^2$ coupled to a standard 12VDC 120 mm fan. Seven K-type probe thermocouples by Omega measure the working fluid temperature at the inlet and outlet of the evaporator and condenser, the liquid saturation temperature in the evaporator, the air temperature at the inlet of the condenser fan and the junction temperature of the devised heating system. Temperature readings are acquired with a Data Translation DT9828 12-bit ADC card. A −1.2bar GEFRAN gauge pressure transducer is connected to the evaporator, acquired by a 12-bit NI USB-6008 card from National Instruments. Thermal power dissipated by the transistor due to Joule effect is acquired by voltage and current readings with a shunt precision resistor, using the abovementioned NI card. Pool boiling curves for HFE 7000 were obtained for PID controlled pressure conditions of 900 mbar. This particular operational pressure condition was chosen due to the fact that for the set-point of 900 mbar the system reaches stable conditions within the widest power range that can be tested in this arrangement: from 50 W to 150 W. After data reduction, the results show that in the abovementioned power range, inner pressure was maintained always within a maximum deviation of 3.12 mbar from set-point and corresponding liquid temperature at 31.3 ˚C in average, among all collected data points, with standard deviation from the average measurements for each point of 0.2 ˚C. The adopted methodology consists on starting every experiment at maximum power, thus maximizing nucleation sites activation and decreases step by step the heat load until 50 W. Each curve is averaged from 4 data sets, for each surface, two built for increasing power steps and two for decreasing power steps. Typical uncertainty of the instrumentation used was ± 1 ˚C for the temperature measurements, ± 15 mbar for the pressure measurements and ± 1.2% for the evaluation of the imposed heating power.

On the other hand, single droplets with a fixed diameter $D_0$ = 3.0 mm ± 0.2 mm are formed at the tip of a needle and fall on the test surfaces by action of gravity. The impact velocity is set at $U_0$ = 2.0 m·s$^{-1}$. The droplets impact perpendicularly to the surface. The relative uncertainty in evaluating the impact velocity is lower than 3%. The liquid is fed to the needle by a syringe pump, being kept at ambient temperature (20 ˚C ± 3 ˚C). The test surfaces are accommodated on an aluminium base inside which 2 cartridge heaters of 80 W are placed. The temperature of the test surfaces is PID controlled with an uncertainty of ± 1 ˚C. Care is taken to assure that the surface is dry and recovers its initial temperature between droplet impacts. The experiments were performed using smooth aluminium and superhydrophobic surfaces, submitted to several heating conditions: $T_{surface}$ = 40 ˚C – 60 ˚C – 80 ˚C – 100 ˚C – 110 ˚C. Droplet morphology at impact is recorded with a high-speed camera, Phantom v4.2 with a frame rate of 1400fps@ 512 px × 512 px. For the optical configuration used here the spatial resolution was 25 m·pixel$^{-1}$. Simultaneous but not synchronised IR images of the temperature field in the droplet and at the liquid interface with the surface were obtained using a high-speed infrared (IR) camera ONCA-MWIR-InSb from Xenics

(ONCA 4696 series), with a frame rate of 1400 fps and a typical resolution of 320 px × 256 px. The investigated region of interest was 105 px × 104 px, corresponding to a pixel size of (30 × 30) μm$^2$. An accuracy of ± 2 ˚C is obtained for the optical configuration used here. However, this camera has a very high thermal sensibility < 17 mK which allows a clear definition of temperature gradients, that are the main focus of the analysis presented in section **3.3**. Water is used here due to its high infrared emissivity ($\varepsilon$ = 0.95).

## 3 Results and discussion

### 3.1 Complex surfaces applied to pool boiling: the effect of superhydrophobicity

Pool boiling experiments are performed with distilled and degassed water on a smooth aluminium alloy hydrophilic and on superhydrophobic (bioinspired) aluminium alloy surfaces, prepared as described in section **2.1**. The hierarchical and organized topography of the Lotus leaf bioinspired surfaces is composed by crater-like micro-cavities with a diameter varying between 100 μm – 200 μm and central distance between them $S$ of 400 μm – 600 μm. The packing of these micro-cavities is not dense. Then, sub-micro scale ripples are observed with a width ranging between 0.1 μm – 2 μm. Any significant change was observed on the morphology of surfaces before and after being modified with DTS. This type of structure is vital to obtain hydrophobic characteristics as studied in detail in Ref. [6]. However, Ref. [6] also shows that the chemistry of the surface plays an important role, being responsible to increase the contact angle by more than 20˚. The resulting boiling curves, taken at a constant pressure of 1 ± 0.0016 bar, are depicted in Fig. 1. The wall superheat is defined as $T_{surface} - T_{sat}$, where $T_{surface}$ is the real temperature of the surface and $T_{sat}$ is the saturation temperature of the liquid.

Following the description reported in the literature, as revised in the Introduction, it was expected that the superhydrophobic surface would promote the onset of boiling to occur at very low superheat (1˚C – 2 ˚C), but then, as the forces acting on the bubbles preclude their release from the surface, promoting their horizontal coalescence, large vapour films should form at relatively low superheats (5˚C – 10 ˚C) insulating the surface and precluding its rewetting[13,39]. Consequently, the heat flux should increase almost linearly with the surface

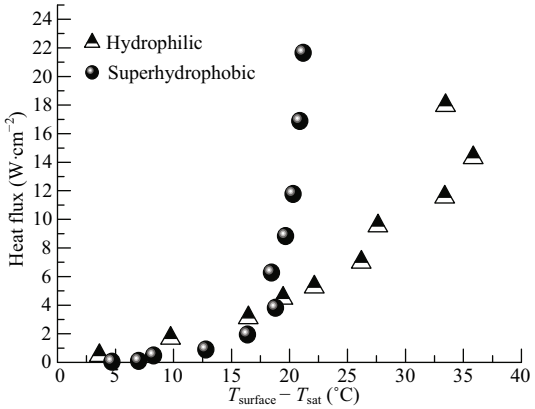


**Fig. 1** Boiling curves obtained for smooth hydrophilic and superhydrophobic (bioinspired) aluminium surfaces.

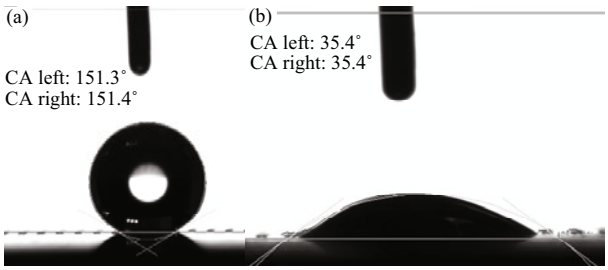


**Fig. 2** Equilibrium contact angle measured. (a) Before; (b) after the boiling experiments.

superheat at much lower slope than that obtained with the hydrophilic (smooth) surface[39]. Such trend is however not observed in Fig. 2. Indeed, the onset of boiling occurs at very low wall superheat for the superhydrophobic surface, but then at 15 ˚C – 18 ˚C of wall superheat, the boiling curve depicts a steep increase in the heat flux, thus resulting in a significantly improved heat transfer performance, when compared to the smooth hydrophilic surface (*i.e.* higher heat fluxes can be removed while keeping the wall superheat low and therefore allowing the surface to be cooled, to remain at low temperatures). Visual observation of the boiling process allows identifying a sudden change in the bubble dynamic mechanisms and in the flow near the surface, which seemed to be rewetted again, as this wall superheat (15 ˚C – 10 ˚C) was achieved. Such phenomenon can only occur if the surface loses its superhydrophobic properties, which means that the durability of the chemical coating was compromised.

To confirm this hypothesis, the equilibrium contact angle was evaluated after the boiling experiments. As shown in Fig. 2, which compares the measured contact angles before and after the boiling experiments, the contact angle steeply decreases from 152˚ (Fig 2a) be-

fore submitted to the water boiling conditions, to 35° (Fig. 2b).

The initial high contact angle and low hysteresis (< 4° as determined in section **2.1**) definitely confirm a stable superhydrophobic regime. The dramatic decrease of the contact angle clearly indicates that the surface has lost its superhydrophobic characteristics after the boiling test. It is worth reminding that for the surface tested here, with the sparser distance between cavities, the increase in the contact angle due to the structuring is minor, of the order of 10° – 20°. Larger contact angles are obtained with other micro-patterns, as described in section **2.1**, but the chemical coating is the responsible for the superhydrophobic behaviour, being responsible for an increase in the equilibrium contact angle which can be as high as 110°, so much larger than that reported for instance by Ref. [6]. On the other hand, given that there were no obvious changes in the topography before and after the boiling, one may argue that the durability of the chemical coating was compromised, most probably due to the violent and invasive nature of the nucleation and bubble dynamics processes, but also due to the high temperatures achieved during the test (between 100 °C and 150 °C). This fabrication method is therefore inadequate for pool boiling applications involving such high temperatures. Alternative techniques are currently being explored. A strong increase in the contact angle of more than 100° based on the use of a chemical coating and without a significant modification in the surface topography has been recently reported for instance by Refs. [40] and [41], so the trend mentioned above is not in disagreement with the most recent literature. The improved heat transfer performance of the superhydrophobic surface after the coating failure can be explained based on the fact that as the coating failure occurs, the surface depicts a random biphilic pattern of hydrophilic/hydrophobic regions, which is expected to combine the advantages of both extreme wetting regimes, thus allowing an effective heat transfer enhancement[11]. Also, visual observation of the boiling process also suggests that this coating failure induces a significant effect on bubble dynamics, allowing the formation and detachment of small bubbles, combined with large bubbles, which facilitates bubble detachment, endorsing the induced fluid motion and surface rewetting, being in line with the observations reported, for instance in Ref. [16]. Finally, besides the coating, the surface was micro-patterned, which is also expected to enhance pool boiling heat transfer, as explained in the Introduction.

Within this context, it is important to analyze now the effect of surface micro-patterning, when the wettability is not taken to extreme (*e.g.* superhydrophobic) scenarios. Following the analysis performed in the previous paragraphs, only micro-patterned surfaces were tested in the electronics cooling system, described in section **2.2**. Due to its low surface tension, HFE7000 wets very well the surface (equilibrium contact angle is close to 0° on all the tested surfaces, both smooth and micro-structured). The surfaces kept the bioinspired pattern as tested in the previous section. However, the distance between the micro-cavities $S$ was systematically varied between 300 mm and 800 mm, following the results reported by Ref. [22]. The boiling curves obtained for HFE7000 on the bioinspired surfaces patterned with micro-cavities are reported in Fig. 3. The results obtained with water are not discussed here, as they were extensively debated in previous work, using similar surfaces, namely in Refs. [22,25,26]. The results obtained with water are however swiftly discussed in the following paragraphs. It is worth reminding that for this set of experiments, the size and depth of the cavities are fixed, so that only the distance between them $S$ is varied. Given that this set-up is designed to serve as a real cooling system for microprocessors, the wall superheat is defined based on the so-called junction temperature ($T_{junction}$) of the die, which is the main parameter to consider, as high values of $T_{junction}$ (typically higher than 85 °C) can damage the microprocessor. For this set of experiments, a real processor was not used, but instead, the heater simulating the thermal behaviour of a

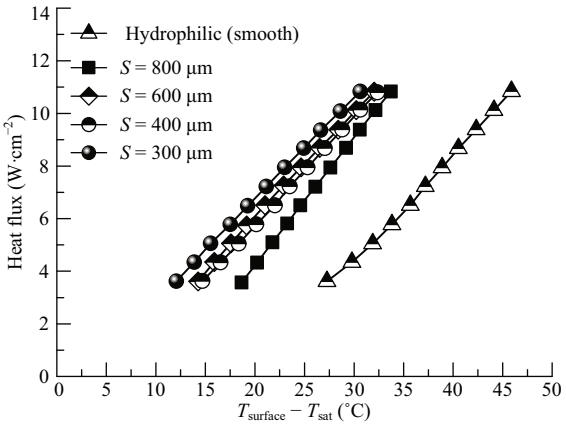


**Fig. 3** Boiling curves obtained for HFE 7000 on the bioinspired micro-patterned surfaces.

microprocessor, as detailed in Ref. [9]. $T_{junction}$ is the temperature of the surface of the main heating element (an IRFP450 transistor with a contact area of 172 mm$^2$ reproducing the die size).

Fig. 3 highlights an overall significant enhanced performance of every micro-patterned surfaces, when compared to the smooth one. This enhanced performance is associated to a significantly higher heat flux, which can be removed by the micro-patterned surfaces, when compared to that removed by the smooth surface, at similar wall superheat. A closer evaluation of the boiling curves depicted in Fig. 3, however, allows distinguishing the performance between the various surfaces. Hence, the surface characterized by the closest and the densest cavities ($S$ = 300 μm) endorses the highest heat fluxes for the same wall superheat, when compared to the other surfaces. On the other hand, the surfaces respectively characterized by $S$ = 400 μm and $S$ = 600 μm depict a similar boiling curve. These results can be interpreted, taking into account the analysis performed in our previous work[22,25,26], obtained for the same fluid boiling over surfaces with similar micro-patterns: increasing the number of cavities, *i.e.* using micro-patterns with smaller values of $S$ leads to two concurrent effects, namely it augments the number of potential nucleation sites, but also favours interaction mechanisms, particularly the coalescence between adjacent nucleation sites. Ref. [25] shows that the negative effects of coalescence were dominant when the so called coalescence number, defined as the average bubble departure diameter with coalescence divided by the average bubble diameter from a single cavity, $D^* = D_{\text{bubble with coalescence}}/D_{\text{bubble without coalescence}} >> 1$. This condition was easily achieved for fluids with large surface tension such as water, for which the highest heat transfer coefficients were achieved at $S$ = 300 μm – 400 μm. This was the distance between cavities found to balance the positive effects of increasing the number of active nucleation sites with the negative effect of a very prominent coalescence between adjacent nucleation sites. Further decreasing the distance between cavities $S$ is reported to lead to a deterioration of the heat transfer coefficient due to intense interaction mechanisms, namely coalescence, which generates large vapour bubbles near the surface[25,26]. The coalescence is less important for fluids like HFE7000, but its effect is not completely negligible[22,25,26]. Furthermore, Refs. [22,26] further suggest that very small distances between cavities contribute to destabilize the induced fluid flow near the surface. Hence the surfaces with the closest cavities ($S$ = 300 μm and $S$ = 400 μm) endorse a larger number of potentially active nucleation sites, but also promote non-negligible interaction effects. This maybe so, since Refs. [22,25,26] report a significant decrease in the heat transfer coefficient corresponding to the degradation of the heat transfer performance, associated to these negative effects of interaction and coalescence mechanisms. This is probably easier to understand when analysing Fig. 4, which depicts a normalized scheme to compare the performance of micro-patterned surfaces, which mainly represents the ratio between the average heat transfer coefficients measured for the micro-patterned surfaces and the heat transfer coefficient obtained with the smooth surface hms/hsmooth, as a function of the distance between cavities $S$.

Fig. 4 gathers the results obtained in the present study with those reported in Ref. [22] for similar experimental conditions (namely for the same fluid and using similar surface micro-patterns). Both data sets follow a similar trend, thus qualitatively confirming the role of the distance between cavities in the enhancement of the heat transfer coefficient. Quantitative discrepancies between them are related to the inherent dependency of the experimental results with particular experimental conditions which are not matched with the current set-up. It is worth mentioning that the enhancement of the heat transfer coefficient is not only linearly affected by the increase in the fluid/surface contact area and the increase of cavity density (obtained for smaller distances $S$), but, as shown in the analysis performed

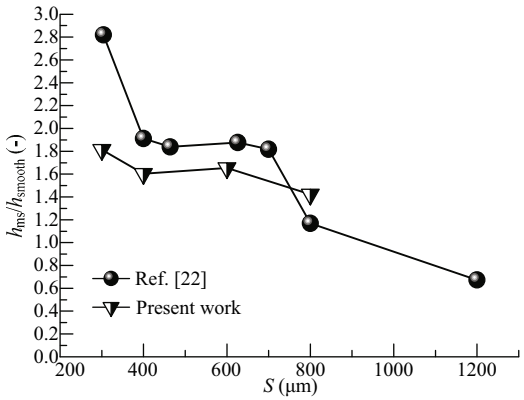


**Fig. 4** Heat transfer coefficient enhancement versus distance between adjacent cavities. Comparison with the results depicted in Ref. [22].

here, also depends on the way the liquid and the surface properties affect the interaction mechanisms and how they are balanced with the increase of active nucleation sites and wetted area. So, care must be taken when using this approach to enhance pool boiling heat transfer. Nevertheless, and in the absence of an effective coating which resists to high temperature variations, surface micro-patterning alone, provides the safest compromise to enhance pool boiling heat transfer.

However, taking these limitations into account the heat transfer coefficient could be increased up to 22.2% for the micro-textured surfaces, with respect to the smooth one.

As aforementioned, the tests discussed within this sub-section were performed in a real pool boiling system which is being developed to cool microprocessors. The results were obtained using the heater that simulates the thermal behaviour of a real microprocessor, so one can control the experimental conditions, namely know the exact value of the imposed heat flux and accurately measure the $T_{junction}$. However, in a recent work, Ref. [9] used this system integrated with the best performing bioinspired surface ($S$ = 300 μm) to cool an Intel i7 2600K (3.4 GHz, Thermal Design Power, $TDP$ = 95 W). For the CPU (Central Processing Unit) stress test conducted (8 threads at 100%), Ref. [9] reports that the cooling system allowed the maximum registered core temperature to be reduced in 26 ˚C more than that registered when using the original Intel fin-fan cooler (part E97378), under the same experimental conditions. These are encouraging results support the use of these surfaces in real case applications.

### 3.2 Complex surfaces applied to spray/droplet impingement

The experiments performed in this last subsection address the dynamic behaviour and heat transfer processes at droplet impact on the bioinspired surfaces, by combining high-speed visualization with time resolved IR thermography. As explained in the Introduction, these experiments address the effect of using the bioinspired surfaces to improve the heat transfer at droplet impact, as an alternative cooling strategy to pool boiling. As for pool boiling, after impact, the droplet spreads on a liquid film over the heated surface, being the spreading motion, the heat transfer process and the possible boiling mechanisms of this thin film also dominated by the

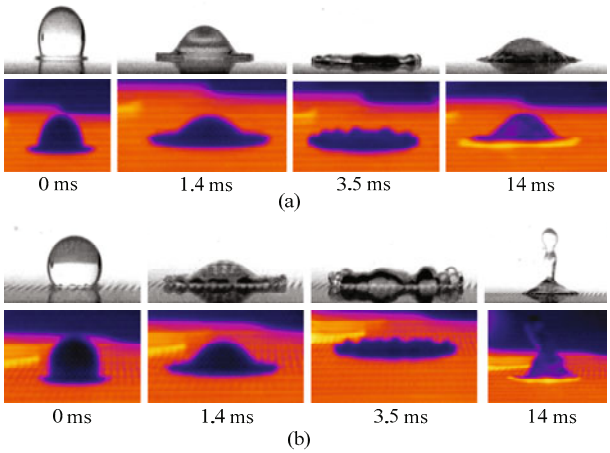


**Fig. 5** Water droplet ($D_0$ = 2.8 mm, $U_0$ = 2 m·s$^{-1}$) impacting on (a) an aluminium alloy hydrophilic surface and (b) a superhydrophobic bioinspired surface heated at $T_{surface}$ = 60 ˚C. The top images are taken with a high-speed camera, while the bottom images are taken with the high-speed thermographic camera.

phenomena occurring at the liquid-solid interface. Particularly, the nucleation scenarios are very similar. Also, there are many similarities regarding the role of wettability in the liquid-solid contact region for droplet spreading and for bubble growth[40,42]. Fig. 5 reports the sequence of high-speed and thermographic images for a water droplet impacting on a smooth hydrophilic aluminium surface (Fig. 5a) and on a superhydrophobic bioinspired surface (Fig. 5b). These results are taken when the surfaces are heated at $T_{surface}$ = 60 ˚C, but a similar behaviour is observed at higher temperatures ($T_{surface}$ = 110 ˚C). $t$ = 0 ms corresponds to the instant of impact. The corresponding temperature profiles, taken in the vertical direction (central region of the droplet) from the region of the liquid-solid interface up to the top of the droplet are shown in Fig. 6. At this stage of the work, these results are to be interpreted mainly from a qualitative point of view. However, the temperature gradients can be associated to the actual dynamic processes that are being observed.

After impact, the droplet spreads until the maximum diameter is reached ($t$ = 14 ms). Given that the characteristic time scale of droplet spreading (tens of ms) is much faster than that of the heat transfer from the surface to the liquid (tens to hundreds of ms) any significant temperature variation is observed in the droplet which remains mainly at ambient temperature. During recoil (for $t$ > 14 ms) one can already observe a temperature increase of the liquid near the surface, given the smaller thickness of the liquid film (called lamella). This

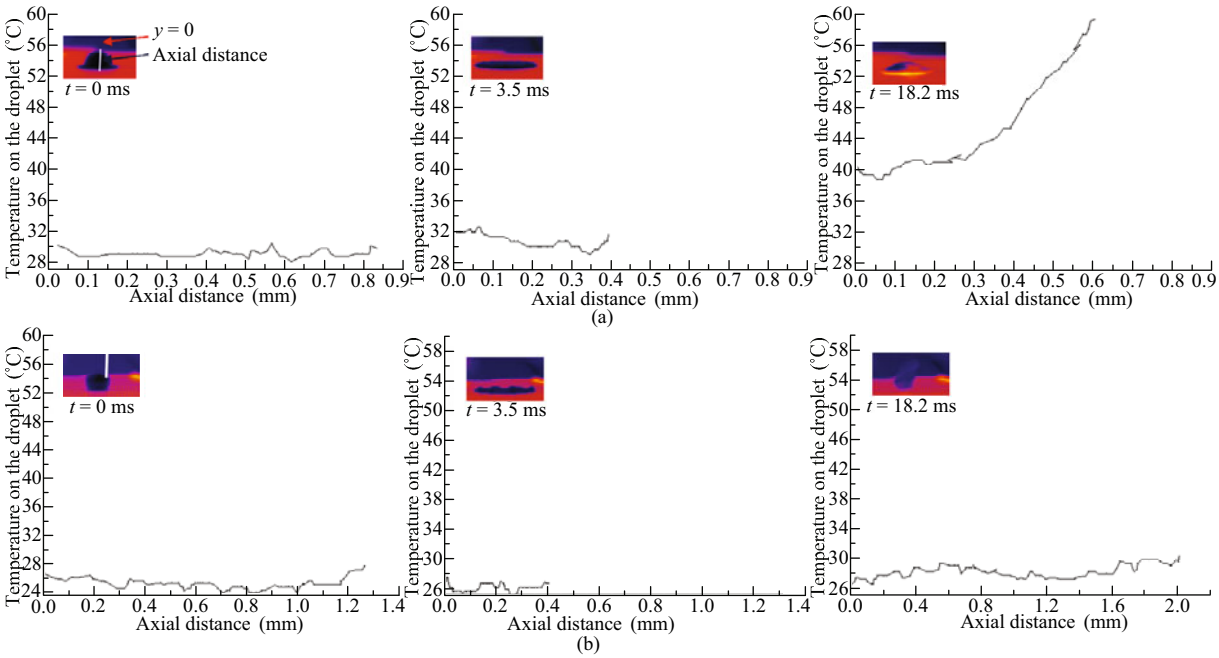


**Fig. 6** Temperature profiles taken at the at the central region of a water droplet ($D_0$ = 2.8 mm, $U_0$ = 2 m·s$^{-1}$), from the surface to the top of the droplet, for various instants after impact. (a) Droplet on the hydrophilic (smooth) surface; (b) droplet on the superhydrophobic bio-inspired surface. Initial surface temperature $T_{surface}$ = 60 ˚C.

is in agreement with the experimental results of Ref. [34] and with the numerical predictions of Ref. [35] for water impacting onto smooth metallic surfaces: given the larger temperature gradient, higher heat fluxes are removed at the liquid-solid interfaces. It should be mentioned that the surface and the lamella are at the same temperature, being the different colours associated to the emissivity values. The camera is calibrated to receive the radiation emitted from the liquid and not from the surface, so the emissivity considered is that of the liquid. After recoiling and the liquid returns to the central region of the droplet, it attains an equilibrium diameter slowly oscillating in a quasi-static behaviour (from $t$ = 18.2 ms to $t$ = 538 ms). At this stage, heat is removed with a lower rate (as the velocity of the flow is very low) and the droplet "bulk" increase in temperature only after a considerable amount of time ($t$ = 538 ms), until reaching a nearly homogeneous temperature distribution. Additional information can however be taken from the IR images taken to the bottom of the surface, as depicted in Fig. 7 $r$ = 0 corresponds to the central point of impact (center of the droplet). As the surfaces are too thick, the images taken beneath the surface are taken using a thin stainless steel foil (with a thickness of 20 μm) heated by Joule effect.

Interesting features are observed here looking at the temperature variation along the direction of the droplet radius, on the surface, in the region impacted by the droplet, which highlights significant temperature differences that may actually be observed between the surface and the droplet, under the transition heat transfer conditions occurring during droplet spreading. Hence, at earlier instants after impact (between $t$ = 0 ms and $t$ = 1.4 ms), a cooling point is noticeable at the central region $r$ = 0 mm (the region of impact) which is a stagnation point. Afterwards, the central region of the surface contacting with the bulk liquid of the droplet remains cooler, as expected and larger gradients can be observed at the liquid-solid interface (identified in Fig. 7b), which are responsible for the high local heat fluxes removed at this region, as reported for instance by Refs. [31,33,34]. The temperature variation in the radial direction of the droplet is quite in good agreement with that reported by Ref. [33], except that the temperature recover from lower temperatures (at the point of impact) to the rim of the higher temperatures at the rim of the lamella occurs at a less steeper slope in the present work than when compared with that of Ref. [33]. This can be related to the fact that Ref. [33] measures the temperature of the droplet (at the interface with the surface) with a thermocouple, while the present work depicts temperature information of the surface, taken from IR

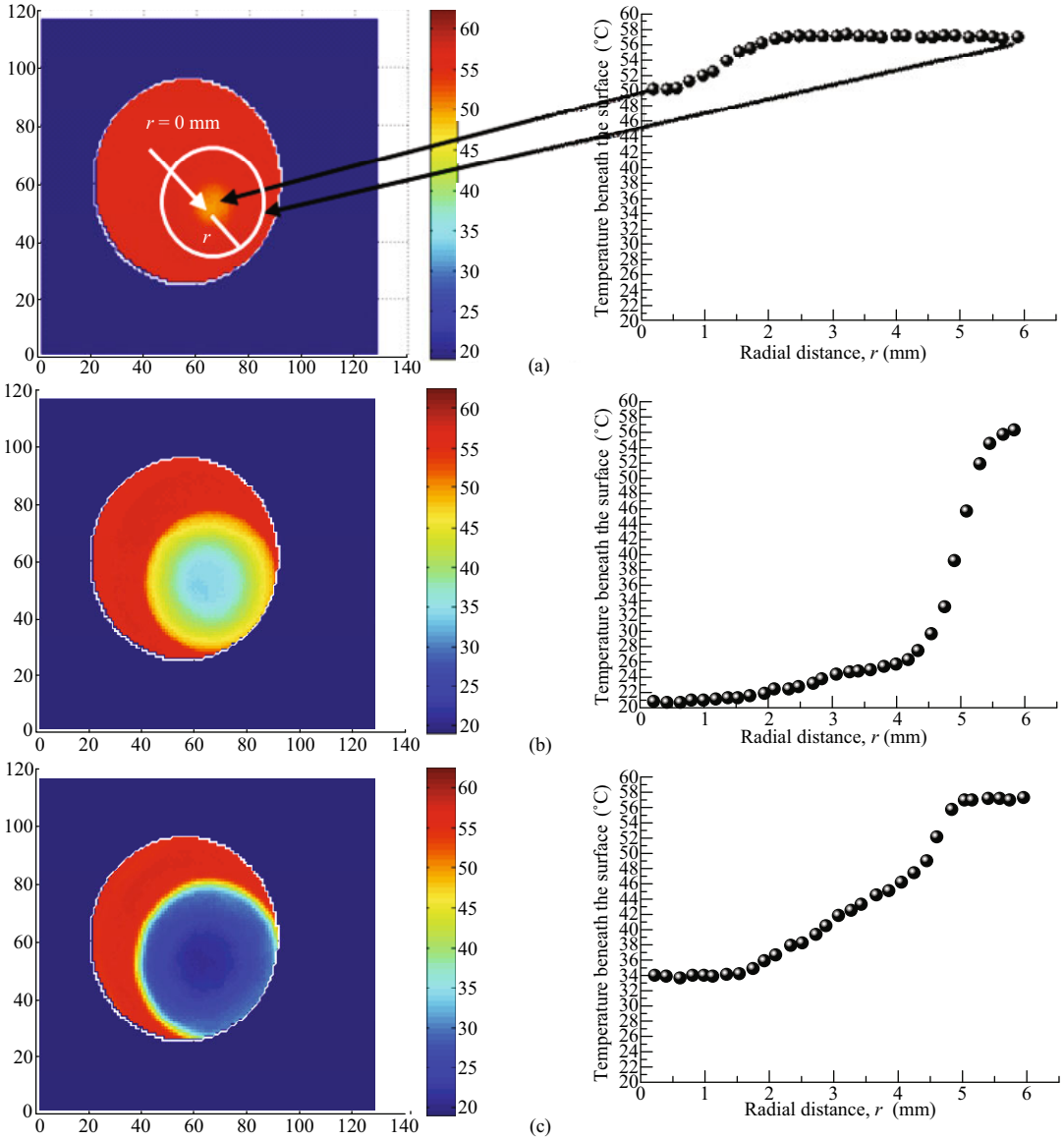


**Fig. 7** Temperature profile in the radial direction (from the center to the periphery of the droplet) for different time steps during the spreading of a water droplet, $D_0$ = 2.8 mm, $U_0$ = 2 m·s$^{-1}$. The surface is a smooth stainless steel surface (20 μm thick). (a) $t$ = 0 ms; (b) $t$ = 1.4 ms; (c) $t$= 15.4 ms. Initial surface temperature $T_{surface}$ = 60 ˚C.

analysis. On the other hand, Ref. [35] reports a faster recover from of the temperature at the central point of impact. Hence, while Ref. [35] reports that the temperature recovers up to the initial value (60 ˚C) nearly 20 ms – 30 ms after the impact, in the present work, such recover only occurs nearly 156 ms after impact. However, it is worth mentioning that Ref. [35] presents a simulation of the temporal variation of the interfacial temperature at the droplet, while the present work is looking at the surface temperature.

The behaviour of the impinging droplet on a superhydrophobic surface is completely different from the one described in the previous paragraphs. In this case, the pinning of the contact line is reduced and the energy dissipation by surface friction is also reduced. As a result, the spreading is much faster when compared to that observed for the smooth surface and the maximum diameter is attained much earlier ($t$ = 3.5 ms). Subsequently, the droplet has an excess of surface energy at its maximum extent, thus suffering a strong recoil followed by a complete rebound at $t$ = 18.2 ms. The short time scale of the droplet dynamics and the small contact area between the droplet and the surface significantly decrease the heat transfer from the surface to the droplet, which remains at ambient temperature during the entire spreading and recoiling processes, even at the liquid-

solid interface. The droplet falls back to the surface, nearly at $t$ = 49 ms and continues oscillating until reaching equilibrium, a very long time after impact ($t$ = 1327 ms). Only then one can observe the temperature increase in the droplet. Besides the particular dynamic behaviour, which precludes the heat transfer between the surface and the droplet, the heterogeneous regime characteristic of superhydrophobic surfaces endorses air entrapment within the roughness groves, acting as an insulating layer. This particular scenario facilitates the durability of the coating. Naturally that the superhydrophobic wetting regime is not adequate to cooling applications, based on droplet impingement. However, it allows the droplets to impact and rebound without a significant heating, which is important in some industrial processes (*e.g.* keeping lubrication and cooling in metallurgical applications) under safe working conditions.

## 4 Conclusion

The work presented here addresses the potential to use Lotus leaf bioinspired surfaces in applications involving heat transfer with phase change, namely pool boiling and spray impingement. The results show that in pool boiling applications the coating of the superhydrophobic surfaces cannot withstand the harsh conditions associated to the high temperatures (> 100 ˚C) and the violent boiling process involved in the pool boiling of water. However, as the coating breaks, the bioinspired hierarchical topography of the surface is responsible for a significant improvement in the pool boiling heat transfer. Hence, for pool boiling of HFE 7000, which has a much lower saturation temperature (~34 ˚C), the bioinspired structures promote an increase of the heat transfer coefficient of 22.2%, when compared to that obtained with a smooth surface. In this case, the heat transfer enhancement is governed by the distance between adjacent cavities, which allows controlling the interaction mechanisms and the flow near the surface. Droplet impingement was studied for smooth hydrophilic and superhydrophobic bioinspired surfaces, heated between 60 ˚C and 100 ˚C, as a simplified configuration of cooling systems based on spray impingement. For this part of the work, an innovative diagnostic technique is proposed, the time resolved IR thermography, which is combined with high-speed visualization and image post-processing to provide additional information on the actual temperature fields and on the heat transfer processes occurring during droplet spreading. The results do not support the use of superhydrophobic surfaces to enhance the heat transfer for this application, but reveal great potential for situations in which the rebounding droplets should not become too hot (*e.g.* in some metallurgical applications).

## Acknowledgement

The authors are grateful to Fundação para a Ciência e a Tecnologia (FCT) for partially financing the research under the framework of the project RECI/EMS-SIS/0147/2012 and for supporting Miguel Moura with a research fellowship. The authors also acknowledge FCT for financing the Post-Doc fellowship of Ana Sofia Moita (SFRH/BPD/109260/2015) and the PhD scholarship (SFRH/BD/88102/2012) of Emanuele Teodori. The authors also thank to BIOAPPRONFS WETT - BIOMIMETIC APPROACHES OF NATURAL FUNCTIONAL SURFACES WITH HIERARCHICAL MICRO & NANO STRUCTURE AND THE EXTREME WETTABILITY, Project Marie Curie (FP7-People-2011-IRSES, Ref.: 295224). Finally, the authors acknowledge to the National Natural Science Foundation of China (Nos. 51275555 and 51325501), the 1111 Project (No. B16020)and Science and Technology Development Project of Jilin Province (No. 20150519007JH).

## References

[1] Bhushan B, Jung Y. Natural and biomimetic artificial surfaces for superhidrophobicity, self cleaning, low adhesion and drag reduction. *Progress in Materials Science*, 2011, **56**, 1–108.

[2] Theodorakakos A, Ous T, Gavaises M, Nouri J, Nikolopoulos N, Yanagihara N. Dynamics of water droplets detached from porous surfaces of relevance to PEM fuel cells. *Journal of Colloid and Interface Science,* 2006, **300**, 673–687.

[3] Antonini C, Innocenti M, Horn T, Marengo M, Amirfazli A. Understanding the effect of superhydrophobic coatings on energy reduction in anti-icing systems. *Cold Regions Science and Technology*, 2001, **67**, 68–67.

[4] Liu M J, Zheng Y M, Zhai J, Jiang L. Bioinspired super-antiwetting interfaces with special liquid−solid adhesion. *Accounts of Chemical Research*, 2010, **43**, 368–377.

[5] Liu Y, Liu J D, Li S Y, Han Z W, Yu S R, Ren L Q.

Fabrication of biomimetic super-hydrophobic surface on aluminum alloy. *Journal of Materials Science*, 2014, **49**, 1624–1629.

[6] Pereira P, Moita A S, Monteiro G, Prazeres D M F. Characterization of English weed leaves and biomimetic replicas. *Journal of Bionic Engineering*, 2014, **11**, 346–359.

[7] Malavasi I, Antonini C, Marengo M. Assesing durability of superhydrophobic surfaces. *Surface Innovations*, 2014, **3**, 49–60.

[8] Pal A, Joshi Y K, Beitelmal M H, Patel C D, Wagner T M. Design and performance evaluation of a compact thermosyphon. *IEEE Transactions of Components Packaging and Manufacting Technology*, 2002, **24**, 601–607.

[9] Moura M, Teodori E, Moita A S, Moreira A L N. 2 phase microprocessor cooling system with controlled pool boiling of dielectrics over micro-and-nano structured integrated heat spreaders. 2016 15*th IEEE Intersociety Conference on Thermal and Thermomechanical Phenomena in Electronic Systems* (*ITherm*), Las Vegas, USA, 2016, 378–387.

[10] Panão M, Guerreiro J, Moreira A L N. Microprocessor cooling based on an intermittent multijet spray system. *International Journal of Heat and Mass Transfer*, 2012, **55**, 2854–2863.

[11] Moita A S, Moreira A L N. Drop impacts onto cold and heated rigid surfaces: Morhphological comparisons, disintegration limits and secondary atomization. *Inernational Journal of Heat and Fluid Flow*, 2007, **28**, 755–752.

[12] Kim J. Spray cooling heat transfer: The state of the art. *International Journal of Heat and Fluid Flow*, 2007, **28**, 753–767.

[13] Malavasi I, Bourdon B, Di Marco P, De Coninck J, Marengo M. Appearance of a low superheat "quasi-Leidenfrost" regime for boiling on superhydrophobic surfaces. *International Communications in Heat and Mass Transfer*, 2015, **63**, 1–7.

[14] Takata Y, Hidaka S, Kohno M. Effect of surface wettability on pool boiling:enhancement by hydrophobic coating. *International Journal of Air-Conditioning and Refrigeration*, 2012, **20**, 1150003.

[15] Betz A, Jenkins J, Kim C, Attinger D. Boiling heat transfer on superhydrophobic, superhydrophilic, and superbiphilic surfaces. *International Journal of Heat and Mass Transfer*, 2013, **57**, 733–741.

[16] Teodori E, Palma T, Valente T, Moita A S, Moreira A L N. Bubble dynamics and heat transfer for pool boiling on hydrophilic, superhydrophobic and biphilic surfaces. *Journal of Physics*: *Conference Series*, 2016, **745**, 032132.

[17] Poniews M E, Thome J R. *Nucleate Boiling on Micro-Structured Surfaces*, Heat Transfer Research, Inc. (HTRI), College Station, USA, 2008.

[18] Zhang X, Zhang P Y, Wu Z S, Zhang Z J. Facile fabrication of stable superhydrophobic films on aluminium substrates. *Journal of Materials Science*, 2012, **47**, 2757–2762.

[19] Atsushi H, Cheng D F, Yagihashi M. Hydrophobic/superhydrophobic oxidized metal surfaces showing negligible contact angle hysteresis. *Journal of Colloid and Interface Science*, 2012, **353**, 582–587.

[20] Liu W, Luo Y, Sun L, Wu R, Jiang H, Liu Y. Fabrication of the superhydrophobic surface on aluminum alloy by anodizing and polymeric coating. *Applied Surface Science*, 2013, **264**, 872–878.

[21] Hikita M, Tanaka K, Nakamura T, Kajivama T, Takahara A. Super-liquid-repellent surfaces prepared by colloidal silica nanoparticles covered with fluoroalkyl groups. *Langmuir*, 2000, **16**, 7299–7302.

[22] Teodori E, Moita A S, Moreira A L N. Characterization of pool boiling mechanisms over micro–patterned surfaces using PIV. *International Journal of Heat and Mass Transfer*, 2013, **66**, 261–270.

[23] Nimkar N D. Effect of nucleation site spacing on the pool boiling characteristics of a structured surface. *International Journal of Heat and Mass Transfer*, 2006, **42**, 2829–2839.

[24] Yu C K, Lu D C, Cheng T C. Pool boiling heat transfer on artificial micro-cavity surfaces in dielectric fluid FC-72. *Journal of Micromechanics and Microengineering*, 2006, **16**, 2092–2099.

[25] Moita A S, Teodori E, Moreira A L N. Enhancement of pool boiling heat transfer by surface micro-structuring. *Journl of Physics*: *Conference Series*, 2012, **395**, 012175.

[26] Moita A S, Teodori E, Moreira A L N. Influence of surface topography in the boiling mechanisms. *International Journal of Heat and Fluid Flow*, 2015, **52**, 50–63.

[27] Moita A S, Moreira A L N. Scaling the effects of surface topography in the secondary atomization resulting from droplet/wall interactions. *Experiments in Fluids*, 2012, **52**, 679–695.

[28] Moreira A L N, Moita A S, Panão M R. Advances and challenges in explaining fuel spray impingement: How much of single droplet impact research is useful? *Progress in Energy and Combustion Science*, 2010, **36**, 554–580.

[29] Rioboo R, Voué M, Vaillant A, De Coninck J. Drop impact on porous superhydrophobic polymer surfaces. *Langmuir*, 2008, **24**, 14074–14077.

[30] Marengo M, Antonini C, Roisman I V, Tropea C. Drop

collision with simple and complex surfaces. *Currrent Opinion in Colloid and Interface Science*, 2011, **16**, 292–302.

[31] Strotos G, Aleksis G, Gavaises M, Nikas K, Nikolopoulos N, Theodorakakos A. Non-dimensionalisation parameters for predicting the cooling effectiveness of droplets impinging on moderate temperature solid surfaces. *International Journal of Thermal Science*, 2011, **50**, 698–711.

[32] Moita A S, Herrmann D, Moreira A L N. Fluid dynamic and heat transfer processes between solid surfaces and non-Newtonian liquid droplets. *Applied Thermal Engineering*, 2015, **88**, 33–46.

[33] Pasandideh-Fard M, Aziz S D, Chandra S, Mostaghimi J. Cooling effectiveness of a water drop impinging on a hot surface. *International Journal of Heat and Fluid Flow*, 2001, **22**, 201–210.

[34] Healy W M, Hartley J G, Abel-Kalik S I. On the validity of the adiabatic spreading assumption in droplet impact cooling. *International Journal of Heat and Mass Transfer*, 2001, **44**, 3869–3881.

[35] Shen J, Graber C, Liburdy J, Pence D, Narayanan V. Simultaneous droplet impingement dynamics and heat transfer on nano-structured surfaces. *Experimental Thermal and Fluid Science*, 2010, **34**, 496–503.

[36] Tartarini P, Corticelli M, Tarozzi L. Dropwise cooling: Experimental tests by infrared thermography and numerical simulations. *Applied Thermal Engineering*, 2009, **29**, 1391–1397.

[37] Girard F, Antoni M, Sefiane K. Infrared thermography investigation of an evaporating sessile water droplet on heated substrates. *Langmuir*, 2010, **26**, 4576–4580.

[38] Kim H, Bungiorno J. Detection of liquid–vapor–solid triple contact line in two-phase heat transfer phenomena using high-speed infrared thermometry. *International Journal of Multiphase Flow*, 2011, **37**, 166–172.

[39] Moita A S, Moreira A L N. Influence of surface properties on the dynamic behaviour of impacting droplets. 9*th International Conference on Liquid Atomization and Spray Systems – ICLASS* 2003, *Sorrento*, *Italy*, 2003.

[40] Teodori E, Valente T, Malavasi I, Moita A S, Marengo M, Moreira A L N. Effect of extreme wetting scenarios on pool boiling conditions. *Applied Thermal Engineering*, 2017, **115**, 1424–1437.

[41] Moita A S, Laurência C, Ramos J A, Prazeres D M F, Moreira A L N. Dynamics of droplets of biological fluids on smooth superhydrophobic surfaces under electrostatic actuation. *Journal of Bionic Engineering*, 2016, **13**, 220–234.

[42] Moita A S, Moreira A L N. Scaling the effects of surface topography in the secondary atomization resulting from droplet/wall interactions. *Experiments in Fluids*, 2012, **52**, 679–695.